ISSN (e): 2250 – 3005 || Volume, 09 || Issue, 3|| March – 2019 ||
International Journal of Computational Engineering Research (IJCER)

# Dynamic Mechanical Properties Analysis of High Nitrogen Steels

Avaya Kumar Baliarsingh, *Department of Mechanical Engineering, Aryan Institute of Engineering & Technology, Bhubaneswar*
Subhasis Sarkar, *Department of Mechanical Engineering, NM Institute of Engineering & Technology, Bhubaneswar*
Sidharth Pradhan, *Department of Mechanical Engineering, Capital Engineering College, Bhubaneswar*
Rajaram Sahu, *Department of Mechanical Engineering, Raajdhani Engineering College, Bhubaneswar*

***ABSTRACT:*** *Reliable dynamic mechanical properties of high nitrogen steels are necessary for the design and assessment of armor structures subject to impact and blast. A series of experiments, based on Hopkinson bar techniques, were conducted and described in this study. The dynamic compression, tensile and shear properties of high nitrogen steel had been tested, and the stress-strain curves under high strain rates were obtained. The results have been showed as follows: High nitrogen steel has a remarkable strain rate strengthening effect. Compared to the static curves, the constitutive curves of dynamic tension and compression move upper. The dynamic compressive yield strength of high nitrogen steel increases first and then decreases with the increase of strain rate, and the yield strength varies in the range of 1465 e1549 MPa within the range of 1147e2042 $s^{-1}$ strain rate; The tensile strength of high nitrogen steel increases with the increase of strain rate. When the strain rate is greater than 1341 $s^{-1}$, the tensile strength will not increase and the curve tends to be gentle. The pure shear yield strength of the high nitrogen steel is above 800 MPa.*
***KEYWORDS:*** *High nitrogen steels Hopkinson bar Dynamic compression Dynamic tension Dynamic shear*

## I. INTRODUCTION

Armor steel is the main structural material for the bodywork, turret and additional armor of tanks and armored vehicles, which has good strength, toughness, ballistic performance and good technological performance [1e3]. For a long time, the medium

carbon and low alloy series by increasing the carbon content and using the corresponding heat treatment methods to improve the ballistic performance are used in armor steels at home and abroad [4,5]. High nitrogen steels have been studied and applied abroad since 1960s. And in 1990s, further research on high nitrogen steel has added a new way to the development of armor steel [6]. The strength of high nitrogen steel under the impact of high strain rate is obviously improved. When the projectile penetrates, the target of high nitrogen steel has strong impact hardening, which improves the ballistic performance of high nitrogen steel [7,8]. More than ten years of researches have been carried out in the field of high nitrogen steel abroad, which has already been applied in the field of national defense and military industry, especially in armor pro- tective materials [9]. Therefore, it is necessary to study the dynamic mechanical properties of high nitrogen steels. In this paper, a series of experiments, based on Hopkinson bar techniques, were con- ducted and the dynamic properties of high nitrogen steel had been obtained, which could support the design and assessment of armor structures.

## II. EXPERIMENT

*Experimental materials*

The raw material used in the experiment was 20 mm thickness nitrogen austenitic steel plate. The chemical composition was shown in Table 1. The quasi-static compression and tension stress-strain curves of high nitrogen steel were shown in Figs. 1 and 2. They showed that the compression yield stress and tension yield stress of this material under quasi-static test are about 900 MPa and 1000 MPa respectively.

*Experimental method*

Dynamic tests of high nitrogen steel were carried out on the

Table 1
Chemical composition of high nitrogen steel (u/%).

| Element name | N | C | Mn | Ni | Cr | Mo | Cu | W |
|---|---|---|---|---|---|---|---|---|
| Percentage/% | 0.88 | 0.030 | 19.28 | 2.01 | 19.32 | 0.0001 | 0.031 | 0.005 |

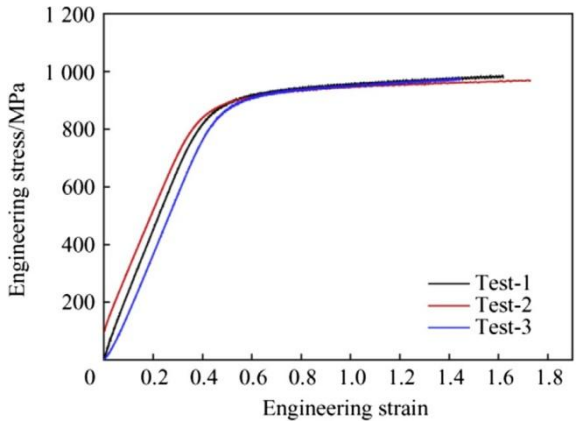


**Fig. 1.** Quasi-static compression stress-strain curve of high nitrogen steel.

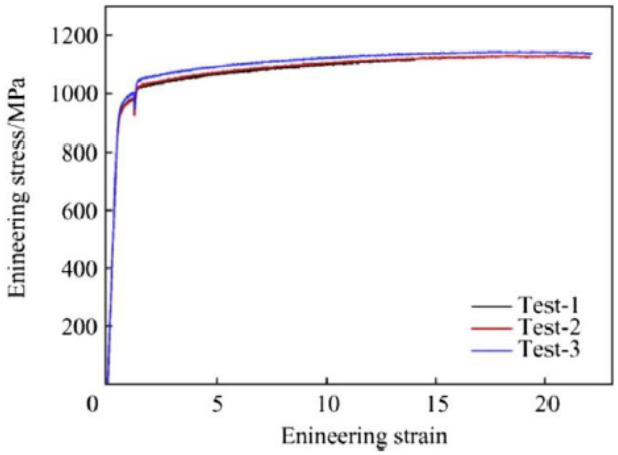


Fig. 2. Quasi-static tension stress-strain curve of high nitrogen steel.

Split- Hopkinson bar at room temperature. It consists of gas gun, incident bar, transmitted bar, striker, buffer bar, shock absorber, and strain gage circuits to measure strain signal in the bars. Figs. 3 and 4 show the Schematic of SHPB and SHTB device.

In this paper, the compression and tension tests were conducted on Hopkison bar which diameter is 16 mm and material is high carbon chromium alloy steel, the shearing tests were conducted on Hopkison bar which diameter is 20 mm and material is LY12 super- hard aluminum alloy. The test specimens were shown in Fig. 5, in which the compression specimens were measured diameter 8 mm 4 mm, the tension specimens were measured diameter 4 mm-gage length 10 mm, the thickness of shearing specimens were 2 mm.

In tension tests, the gas gun launches the tubular striker to impact the incident bar. The transfer flange transfers the incoming elastic compressive stress wave into the elastic tensile stress which travels through the incident bar toward the specimen. When the tensile stress wave propagates into the specimen, it reverberates within the specimen until a nominally homogeneous stress state is achieved. And part of the wave is transmitted through the trans- mitted bar as a tensile wave, the rest is reflected back to the incident bar as a compressive wave. The strain signals were transferred into electrical signals by high dynamic strain indicator, and were recorded by the Multi-channel transient digital recorder. Analo- gously, in compression and shearing tests, through recorder the stress wave travels in the bar to acquire test result.

The test technology of Hopkinson bar is based on two hypoth- esis [10]: the one dimensional

stress hypothesis and the stress uniformity hypothesis. The stress and strain relationship is derived according to the one-dimensional stress wave theory.

The end surface of specimen connected with incident bar is set 1, and the other end surface connected to the transmission bar is set 2. The displacements of interface 1 and 2 are $U_1(t)$ and $U_2(t)$ respectively. It is assumed that the strain signal of tension is negative and compression is positive. So:

$$U_1(t) = -c_0 \int_0^t (\varepsilon_i(\tau) - \varepsilon_r(\tau))d\tau \quad (1)$$

$$U_2(t) = -c_0 \int_0^t \varepsilon_t(\tau)d\tau \quad (2)$$

Where:

$c_0$ elastic wave velocity;
$\varepsilon_i(\tau)$, $\varepsilon_r(\tau)$, $\varepsilon_t(\tau)$ strain signal of incident wave, reflected wave, transmission wave.

It is assumed that the original length and cross section area of the specimen are $l_s$ and $A_s$ respectively, so the average strain in the

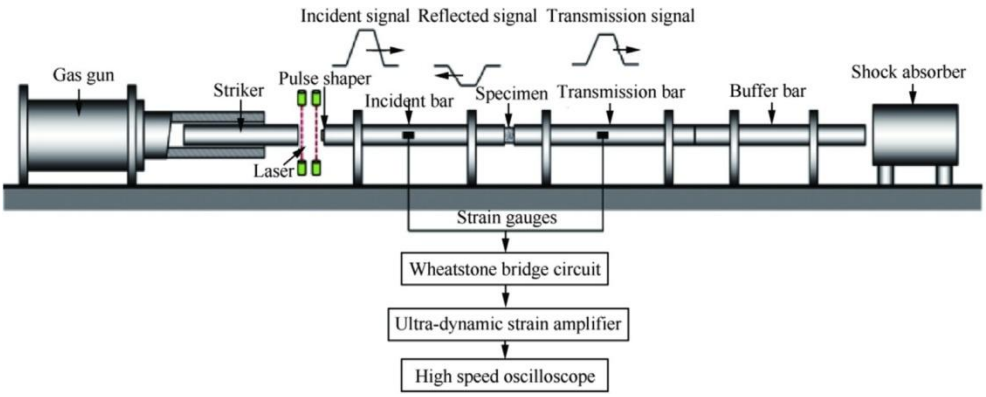


**Fig. 3.** Schematic diagram of SHPB device.

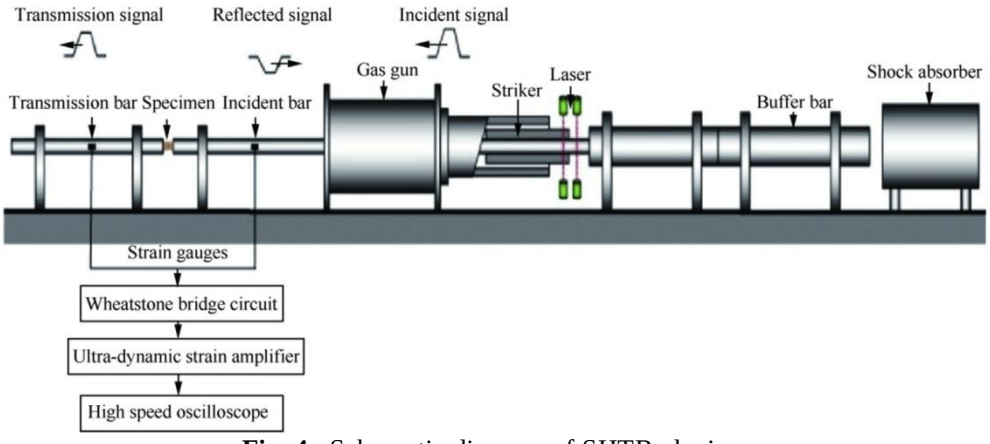


**Fig. 4.** Schematic diagram of SHTB device.

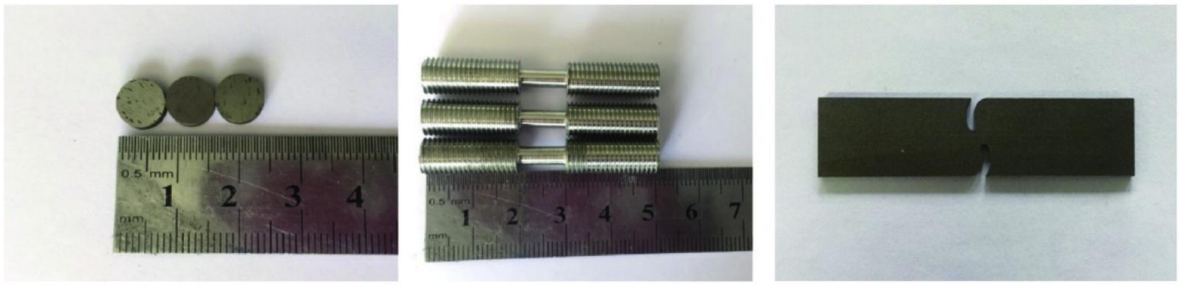

(a) Dynamic compression (b) Dynamic tensile (c) Dynamic shear

**Fig. 5.** The test specimens.

specimen is:

$$\varepsilon(t) = \frac{U_1(t) - U_2(t)}{l_s} = -\frac{c_0}{l_s}\int_0^t (\varepsilon_i(\tau) - \varepsilon_r(\tau) - \varepsilon_t(\tau))d\tau \quad (3)$$

The formula (3) is used to derive the derivative of time, and the strain rate in the sample is obtained.

$$\dot{\varepsilon}(t) = -\frac{c_0}{l_s}(\varepsilon_i(t) - \varepsilon_r(t) - \varepsilon_t(t)) \quad (4)$$

The force of the end face 1 and the end face 2 of the specimen is $P_1(t)$ and $P_2(t)$ respectively. There:

$$P_1(t) = -A_0E(\varepsilon_i(t) + \varepsilon_r(t)) \quad (5)$$

$$P_2(t) = -A_0E\varepsilon_t(t) \quad (6)$$

Where:

$A_0$ cross-sectional area of the bar;
$E$ elestic modulus of the bar.

Average stress in the specimen is:

$$\sigma(t) = \frac{1}{2A_s}(P_1(t) + P_2(t)) \qquad \frac{A_0E}{2A_s}(\varepsilon_i(t) + \varepsilon_r(t) + \varepsilon_t(t)) \quad (7)$$

The above formulas showed how to calculate strain rate, strain and stress in the specimen by incident, reflection and transmission wave.

## III. RESULTS AND DISCUSSION

*The results of dynamic compression experiment*

The results of dynamic compression were analyzed by one dimensional elastic wave theory. At least 3 repeated tests were conducted under each strain rate, and the coherence of each repeated curve was very well. Four dynamic compressive stress- strain curves of high nitrogen steel under different strain rate were shown in Fig. 6. It can be seen from the diagram that high

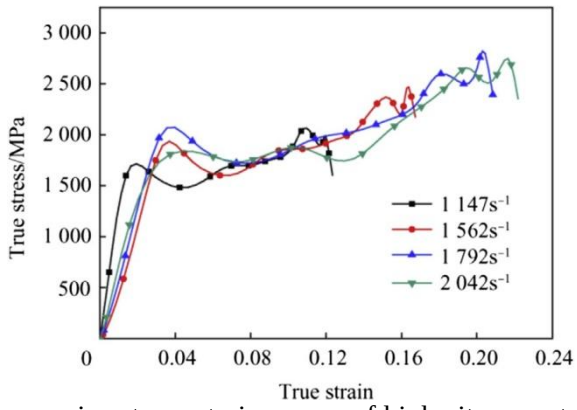


Fig. 6. The dynamic compressive stress-strain curves of high nitrogen steel under different strain rates.

nitrogen steel is very sensitive to the variation rate. When the strain rate is 2042 $s^{-1}$, the yield strength is about 1.5 GPa, which is nearly one time higher than that of quasi-static compression test. In the range of 1147e2042 $s^{-1}$ strain rate, the yield strength of materials
varies in the range of 1465e1549 MPa. On the stress-strain curve, the elastic segment and the plastic hardening section of the real stress-strain curve of each specimen are linearly fitted respectively. The corresponding longitudinal coordinates of the intersection

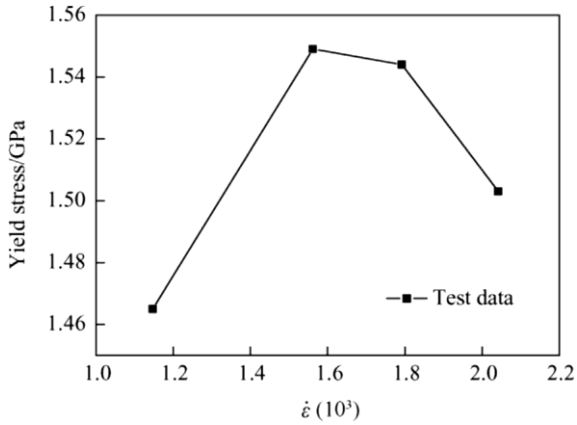


Fig. 7. The relationship between dynamic compressive yield strength and strain rate.

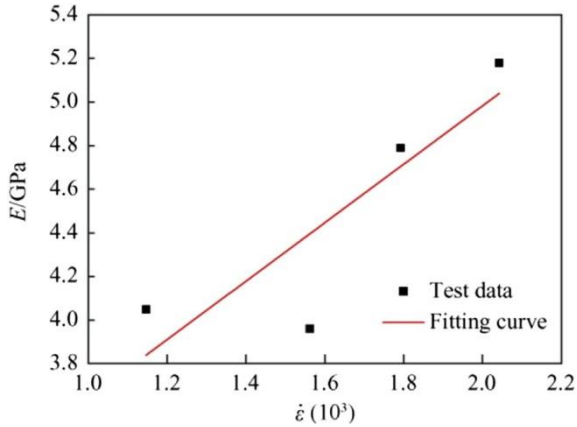


Fig. 8. The relationship between dynamic compressive hardening modulus and strain rate.

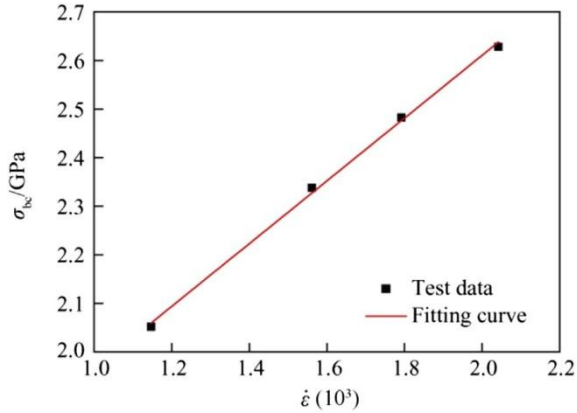


Fig. 9. The relationship between dynamic compressive strength and strain rate.

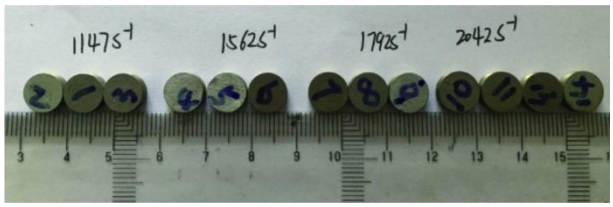


Fig. 10. Specimens after compression.

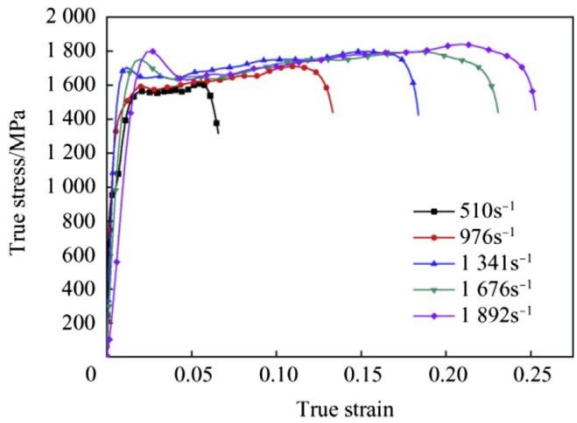


Fig. 11. The dynamic tensile stress-strain curves of high nitrogen steel under different strain rates.

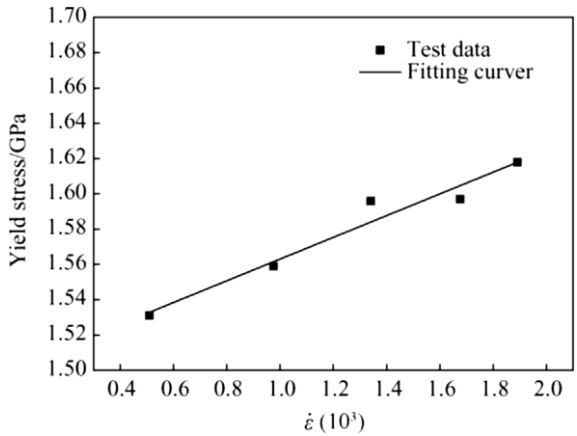


Fig. 12. The relationship between dynamic tensile yield strength and strain rate.

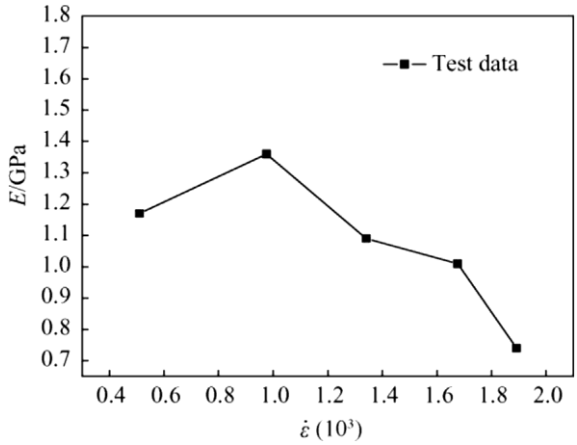


Fig. 13. The relationship between strain strengthening modulus and strain rate.

point of the two straight lines are defined as the yield strength of the material. The slope of the straight line fitted by the plastic section is the strain strengthening modulus of the material. The yield strength, strain hardening modulus and loading strain rate of each specimen were obtained by analyzing and fitting the experimental data. It is shown in Figs. 7e9 that the dynamic compressive yield strength of high nitrogen steel increases first and then de- creases with the increase of strain rate. The strain hardening modulus and compressive strength increase with the increase of strain rate.

Fig. 10 is the specimens after compression. It showed that under tests strain rate the specimens were not crushed after compression. As the increase of loading strain rate, specimens after compression

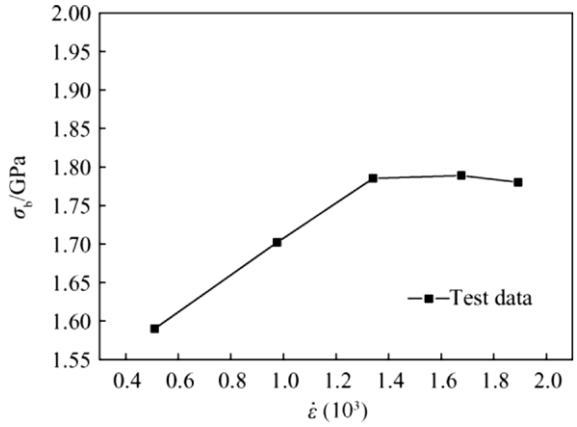


Fig. 14. The relationship between tensile strength and strain rate.

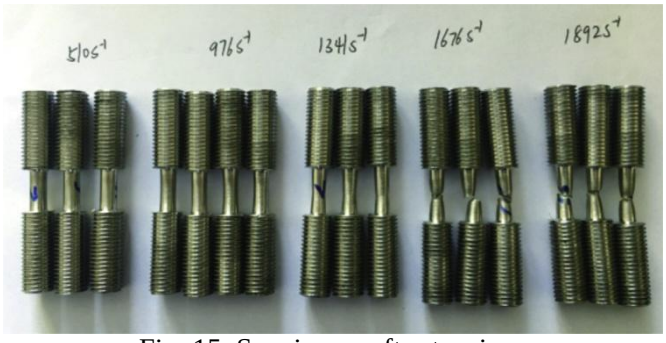


Fig. 15. Specimens after tension.

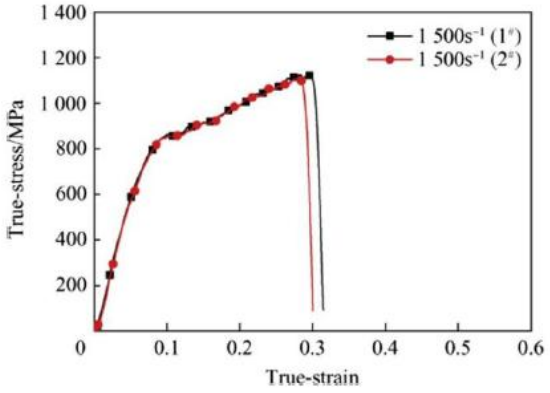


Fig. 16. The real stress-strain curves under 1500 s-1 strain rate.

were thinner, the diameter of which were larger.

*The results of dynamic tensile experiment*

In order to obtain the dynamic mechanical properties of high nitrogen steel accurately, multiple unidirectional dynamic tensile tests were carried out. The dynamic tensile stress-strain curves were shown in Fig. 11. In the range of 510e1892 $s^{-1}$strain rate, the yield strength of high nitrogen steel varies in the range of 1500e1700 MPa, which is higher than the quasi-static tension strengh. Therefore, high nitrogen steel has a remarkable strain rate

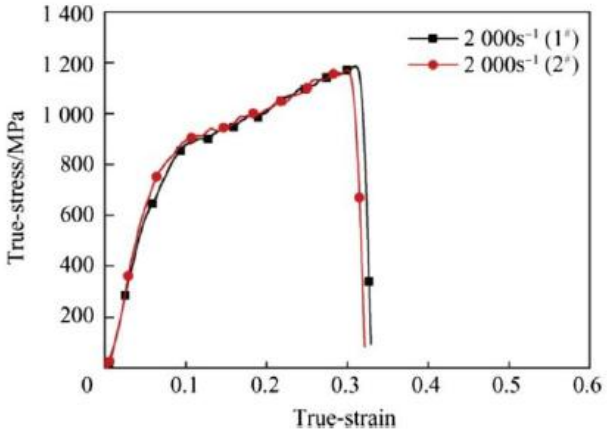


Fig. 17. The real stress-strain curves under 2000 $s^{-1}$ strain rate.

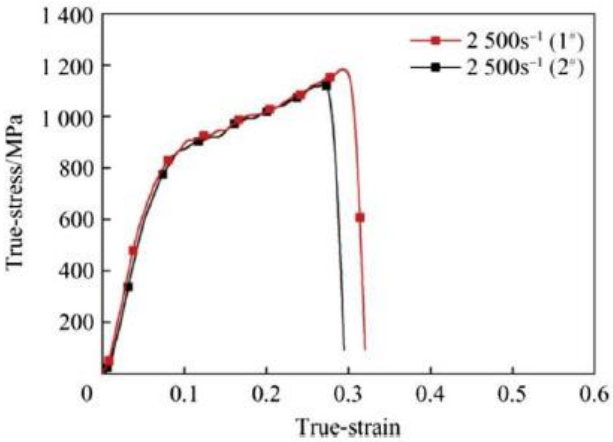


Fig. 18. The real stress-strain curves under 2500 $s^{-1}$ strain rate.

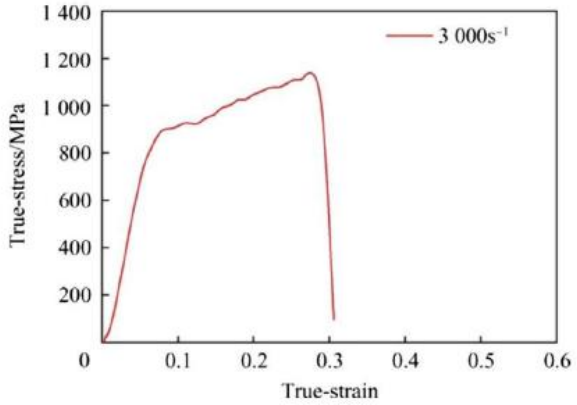


Fig. 19. The real stress-strain curves under 3000 $s^{-1}$ strain rate.

strengthening effect. When the strain rate is 510 $s^{-1}$, 976 $s^{-1}$ and 1341 $s^{-1}$, the tensile specimens of high nitrogen steel do not show the macroscopic fracture, and when the strain rate is 1676 $s^{-1}$ and 1892 $s^{-1}$, the specimens are broken obviously during the tensile loading. It is shown from the Figs. 12e14 that the dynamic tensile

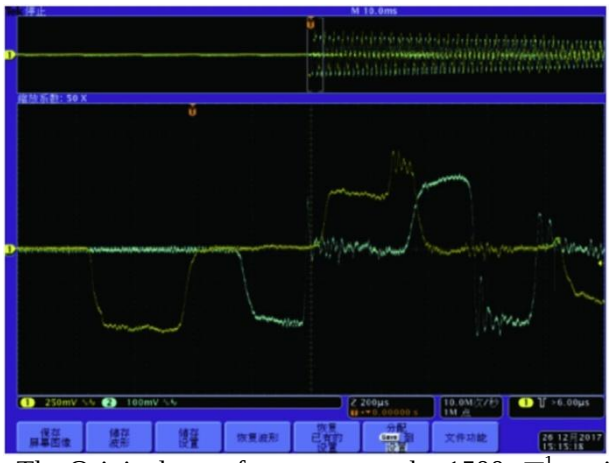

Fig. 20. The Original waveform curve under 1500 $s^{-1}$ strain rate.

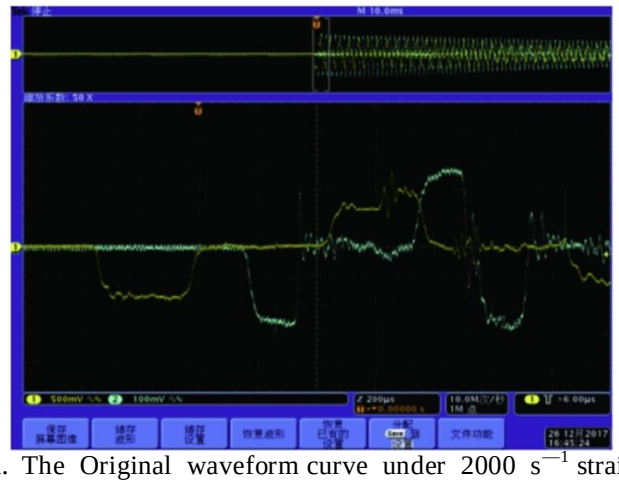

Fig. 21. The Original waveform curve under 2000 $s^{-1}$ strain rate.

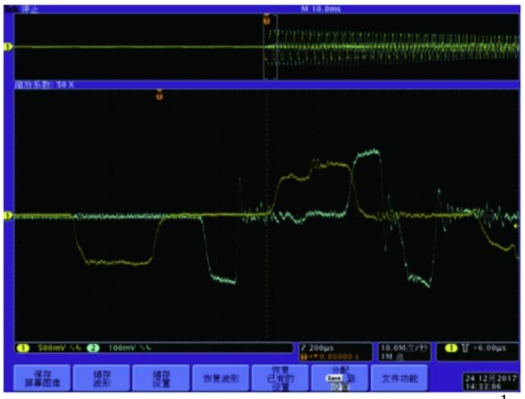

Fig. 22. The Original waveform curve under 2500 $s^{-1}$ strain rate.

yield strength of high nitrogen steel materials increases with the increase of strain rate. The dynamic compressive yield strength of high nitrogen steel first increases and then decreases with the in- crease of strain rate. The strain hardening modulus and compres- sive strength increase with the increase of strain rate. The strain strengthening modulus increases first and then decreases with the strain rate, and the tensile strength increases with the increase of strain rate. When the strain rate is greater than 1341 $s^{-1}$, the tensile strength will not increase, and the curve tends to be gentle.

The specimens after tension were shown in Fig. 15. As the in- crease of strain rate, the necking phenomenon appeared until they

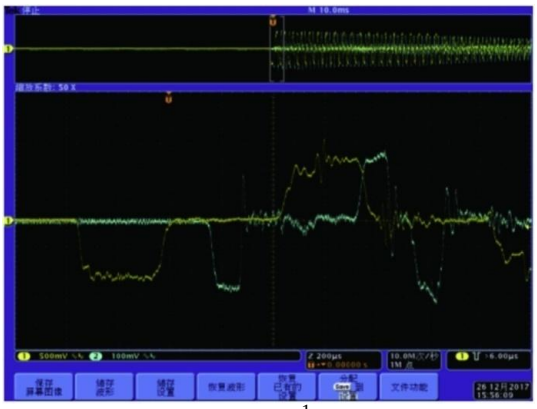

Fig. 23. The Original waveform curve under 3000 $s^{-1}$ strain rate. The photos of frac- ture specimens of high nitrogen steel are shown in Fig. 24.

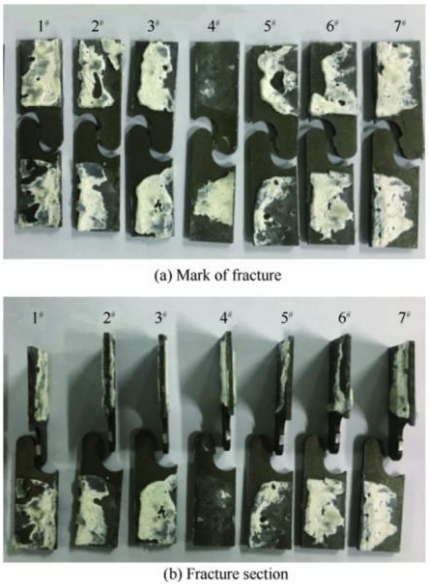


Fig. 24. The specimens after dynamic shear test: (a) mark of fracture; (b) fracture section.

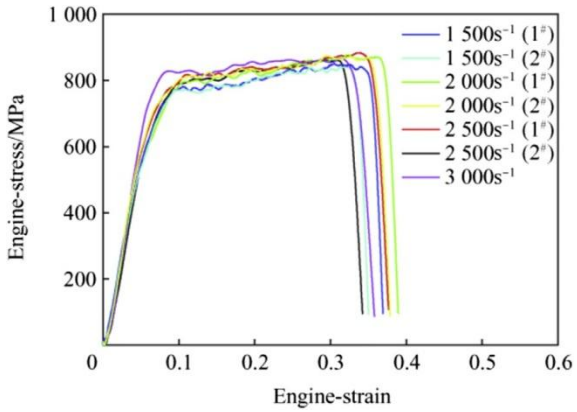


Fig. 25. The engineering stress-strain curves under different strain rates.

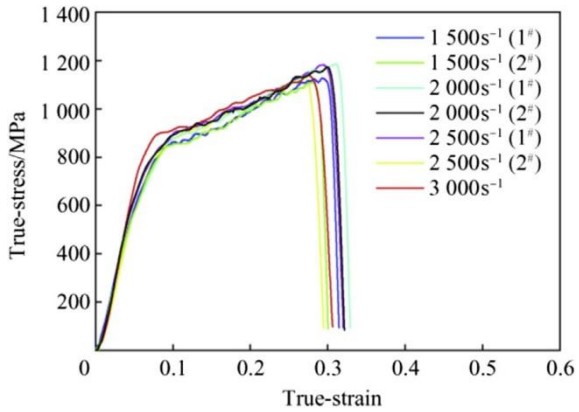


Fig. 26. The real stress-strain curves under different strain rates.

Table 2
The results of dynamic shear experiment.

| Number | Strain rate $\dot{\varepsilon}/s^{-1}$ | Shear strength $\tau_b$/MPa | Uniform elongation $\varepsilon_b$/% | Fracture elongation $A$/% | Energy absorption density $e_A$/MPa |
|---|---|---|---|---|---|
| 1500 $s^{-1}$ (1#) | 1510 | 1124 | 0.282 | 0.314 | 261.7 |
| 1500 $s^{-1}$ (2#) | 1560 | 1109 | 0.280 | 0.300 | 243.7 |
| 1500 $s^{-1}$ (average) | e | 1116.5 | 0.281 | 0.307 | 252.7 |
| 2000 $s^{-1}$ (1#) | 1860 | 1186 | 0.310 | 0.329 | 283.7 |
| 2000 $s^{-1}$ (2#) | 2090 | 1173 | 0.300 | 0.321 | 277.3 |
| 2000 $s^{-1}$ (average) | e | 1179.5 | 0.305 | 0.325 | 280.5 |
| 2500 $s^{-1}$ (1#) | 2380 | 1183 | 0.294 | 0.320 | 276.3 |
| 2500 $s^{-1}$ (2#) | 2440 | 1128 | 0.271 | 0.295 | 240.7 |
| 2500 $s^{-1}$ (average) | e | 1155.5 | 0.2825 | 0.3075 | 258.5 |
| 3000 $s^{-1}$ | 3010 | 1139 | 0.275 | 0.306 | 262.2 |

were broken. The critical strain rate of fracture is between 1341 $s^{-1}$ and 1676 $s^{-1}$.

### *3.3. The results of dynamic shear experiment*

The true stress-strain and the original waveform curves of high nitrogen steels at 1500 $s^{-1}$, 2000 $s^{-1}$, 2500 $s^{-1}$ and 3000 $s^{-1}$ strain rates are shown in Figs. 16e23.

The pure shear stress response curves of high nitrogen steel first entered the elastic phase, and then began to enter the shear strengthening stage after reaching the shear yield strength. Until the shear strength was reached, the shear fracture was formed.

The experimental results show that in the range of strain rate 1500 $s^{-1}$ to 3000 $s^{-1}$, the sensitivity of the dynamic shear strength of high nitrogen steel to the variation rate is not strong. The pure shear yield strength of the high nitrogen steel is above 800 MPa, regardless of the engineering stress-strain curve or the real stress- strain curve.

The engineering and real stress-strain curves are shown in Figs. 25 and 26. The engineering stress is the ratio of the applied load to the original cross-sectional area of the gauge interval, and the engineering strain is the ratio between the elongation of the extended gauge and the original length of the gauge interval. The results of dynamic shear experiment under four strain rates are shown in Table 2.

## Ⅳ. SUMMARY

(1) High nitrogen steel has a remarkable strain rate strength- ening effect. Compared to the static curve, the constitutive curve of dynamic tension and compression moved upper.

(2) The dynamic compressive yield strength of high nitrogen steel increases first and then decreases with the increase of strain rate, and the yield strength varies in the range of 1465e1549 MPa within the range of 1147e2042 $s^{-1}$ strain rate.

(3) The tensile strength of high nitrogen steel increases with the increase of strain rate. When the strain rate is greater than 1341 $s^{-1}$, the tensile strength will not increase and the curve tends to be gentle.

(4) The pure shear yield strength of the high nitrogen steel is above 800 MPa.

## REFERENCES

[1]. Manganello SJ, Abbott KH. Metallurgical factors affecting the ballistic behavior of steel targets. J Mater 1972;7(2):231e5.
[2]. Dikshit SN, Kutumbarao VV, undararajan SG. The influence of plate hardness on the ballistic penetration of thick steel plates. Int J Impact Eng 1995;16(2): 293e6.
[3]. Li JQ, Huang DW, Duan ZQ, et al. The study of the properties of adibatic shear bands in high strength armor steel under high velocity penetration. J Ballist 2003;15(3):86e9.
[4]. Edwards MR, Mathewson A. The ballistic properties of tools steels as a po- tential armour plate. Int J Impact Eng 1997;9(4):297e306.
[5]. Manganello SJ, Abbott KH. Metallurgical factors affectiong the ballistic behavior steel targets. J Mater 1972;7(2):231e9.
[6]. Speidel MO, Kowanda C, Diener M. High nitrogen steel 2003. Swiss: Institute of Metallurgy; 2003. p. 63.
[7]. Lach E, Koerber G, Scharf M, et al. Comparision of nitrogen alloyed austenitic steels and high strength armor steels impacted at high velocity. Int J Impact Eng 1999;23:509e17.
[8]. Lach E, Uggowitzer P, Rondot F. Hardening of nitrogen alloyed steels by shock waves. J Phys IV 1997;7:547e52.
[9]. Lach E, Bohmann A, Scharf M, et al. Deformation behavior of Nitrogen-alloyed austenitic steels at high strain tates. Adv Eng Mater 2000;2(11):750e2.
[10]. KOLSKY H. An investigation of the mechanical properties of materials at very high rates of loading. Proc Phys Soc 1949;B62:676e700.